

NASA TM X-55732

AN OZONE MEASUREMENT IN THE STRATOSPHERE AND LOWER MESOSPHERE BY MEANS OF A ROCKET SONDE

BY
ERNEST HILSEN RATH

N67-33732

(ACCESSION NUMBER)

(THRU)

19
(PAGES)

1
(CODE)

TMX-55732

(NASA CR OR TMX OR AD NUMBER)

13
(CATEGORY)

MARCH 1967

NASA

GODDARD SPACE FLIGHT CENTER

GREENBELT, MARYLAND

FACILITY FORM 602

~~X67-14425~~

(ACCESSION NUMBER)

19
(PAGES)

~~NASA TMX 55732~~

(NASA CR OR TMX OR AD NUMBER)

2D
(CODE)

13
(CATEGORY)

**AN OZONE MEASUREMENT IN THE STRATOSPHERE AND
LOWER MESOSPHERE BY MEANS OF A ROCKET SONDE**

by

Ernest Hilsenrath

March 1967

**Goddard Space Flight Center
Greenbelt, Maryland**

PRECEDING PAGE BLANK NOT FILMED.

AN OZONE MEASUREMENT IN THE STRATOSPHERE AND
LOWER MESOSPHERE BY MEANS OF A ROCKET SONDE

by

Ernest Hilsenrath

ABSTRACT

A technique for the measurement of ozone content in the stratosphere and lower mesosphere by means of a rocket sonde has been developed. The measurement is accomplished by an in-situ determination of the ozone mixing ratio as a function of altitude by means of an ozone sensor utilizing a chemiluminescent detector. The atmosphere is sampled by a self pumping method as the sonde is dropped from apogee via a specially designed high altitude parachute. The ozone detector is not absolute and therefore, must be calibrated before the flight. On December 9, 1966, the first ozone sonde was launched at White Sands Missile Range, New Mexico on a Nike Cajun Rocket. The ozone profile was not measured during this flight because of the failure of the parachute to deploy. However, a brief measurement of ozone mixing ratio just over apogee was accomplished. The measurement yielded .80 micrograms/gram and 1.9 microgram/gram at 59 km and 57 km respectively, where apogee was fixed at 60 km. The error in mixing ratio is 35% and because of a tracking failure the error in altitude is ± 5 km.

PRECEDING PAGE BLANK NOT FILMED.

PRECEDING PAGE BLANK NOT FILMED.
CONTENTS

	<u>Page</u>
ABSTRACT	iii
INTRODUCTION	1
THEORY OF OPERATION OF OZONE SENSOR	1
DESCRIPTION OF OZONE SONDE	4
THE INITIAL FLIGHT	11
RESULTS	12
CONCLUSION	15
REFERENCES	15

LIST OF ILLUSTRATIONS

<u>Figure</u>		<u>Page</u>
1	Ozone Sensor Schematic Diagram	2
2	Ozone Sensor Flight Unit	5
3	Ozone Sensor Block Diagram	5
4	Flight Sequence of Events	7
5	Payload Assembly	8
6	Ambient Pressure vs Descent Time	9
7	Rate of Change of Ambient Pressure vs Descent Time	10
8	Ozone Sensor Simulator and Calibrator	11
9	Comparisons of Ozone Concentrations vs Altitude	14

PRECEDING PAGE BLANK NOT FILMED.

AN OZONE MEASUREMENT IN THE STRATOSPHERE AND LOWER MESOSPHERE BY MEANS OF A ROCKET SONDE

INTRODUCTION

In the lower stratosphere, the ozone content is a quasi-conservative property of the atmosphere and can be used in various meteorological studies concerning scales of atmospheric motions. At higher levels, because of the strong absorption by ozone of solar ultraviolet radiation, this atmospheric constituent plays a dominant part in the radiative-thermal budget. Thus ozone measurements in the stratosphere and lower mesosphere yield valuable information in regard to atmospheric structure and dynamics including effects due to absorption and emission of radiation and the interacting chemical processes.

Presently, soundings for ozone content are routinely made via balloon ozone sondes up to 30 kilometers (Hering and Borden, 1965). Total ozone measurements are performed from ground based stations throughout the world in cooperation with the World Meteorological Organization. Recently, a few rocket measurements using optical and chemical techniques have been flown here and abroad.

The experiment described in this paper will allow a day or night measurement of ozone from 65 kilometers to below the ozone peak at 20 kilometers by means of a rocket borne chemiluminescent ozone sonde. The flights can be performed at various stations where measurements will have greatest geophysical significance such as the polar regions during winter. The flights can also be performed in support of future satellite experiments.

THEORY OF OPERATION OF OZONE SENSOR

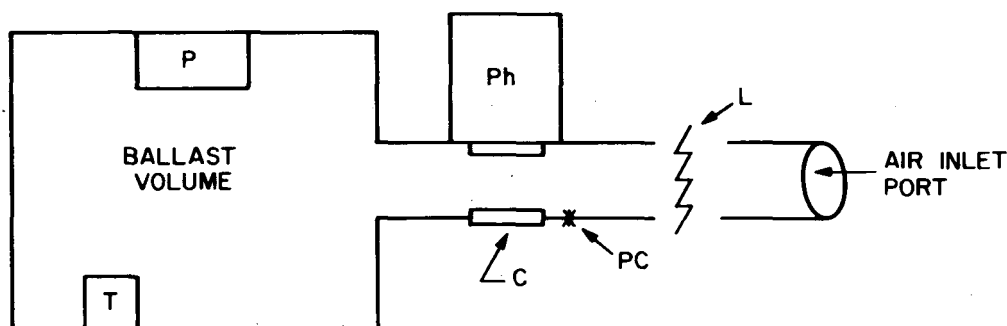
The operation of the ozone sensor can be described in the following manner. Exposure of the chemiluminescent material to ozone causes luminescence. This luminescence is proportional to ozone flux. That is, for a given ozone concentration, the luminescence is proportional to the flow rate of air past the detector, and conversely, at constant flow rates the signal is proportional to the ozone concentration. This relationship is expressed by

$$L \propto [O_3] \times \text{flow rate} \quad (1)$$

where, L , is the light intensity and $[O_3]$ is the ozone concentration. This linear dependence to ozone flux has been amply demonstrated in the laboratory over a specific range of flow rates (Parametrics Final Report, 1963). The ozone sensor has been designed to operate over this linear range, which will be encountered in a parachute descent from 65 km to 20 km.

The sample of air is introduced into the sensor by means of a self pumping mechanism. This mechanism can be described in the following manner (see Figure 1). Consider a ballast chamber or volume that is connected to the external environment by means of an inlet pipe and is in pressure equilibrium with the ambient atmosphere. When the sensor is released from a high altitude and descends through the atmosphere via a parachute, the pressure inside the ballast volume will tend to "keep up" with the increasing external pressure, resulting in a net flow of gas through the inlet pipe. The detector, consisting of the chemiluminescent material and the photometer, is oriented along the tube, thus providing a continuous measurement of the atmosphere for ozone content.

An expression for flow rate can be derived from the equation of state for an ideal gas $PV = nRT$. (This is valid to at least 80 km under our conditions.) The equation



- C — CHEMILUMINESCENT DETECTOR
- L — LIGHT BAFFLE
- P — PRESSURE GAUGE
- Ph — PHOTOMETER
- PC — PHOTOMETER CALIBRATION SOURCE
- T — TEMPERATURE GAUGE

Figure 1—Ozone Sensor Schematic Diagram

$$\begin{aligned}\frac{dn_b}{dt} &= \frac{d}{dt} \frac{(P_b V_b)}{(RT_b)} = \frac{V_b}{R} \left[\frac{1}{T_b} \frac{dP_b}{dt} - \frac{P_b}{T_b^2} \frac{dT_b}{dt} \right] \\ &= \frac{V_b}{RT_b} \left[\frac{dP_b}{dt} - P_b \frac{d(\ln T_b)}{dt} \right]\end{aligned}\quad (2)$$

gives moles of air per second where

n_b = number of moles of air in ballast chamber

P_b = pressure in ballast chamber

V_b = volume of ballast chamber

R = Universal gas constant

T_b = temperature in ballast chamber

The mass flow rate into the ballast chamber is then given by

$$\frac{dm}{dt} = \frac{Mdn_b}{dt} = \frac{MV_b}{RT_b} \left[\frac{dP_b}{dt} - P_b \frac{d(\ln T_b)}{dt} \right]\quad (3)$$

grams of air per second where

m = number of grams of air in ballast chamber

M = molecular weight of air = 28.97.

It is important to note that P_b and T_b in equations (2) and (3) refer only to conditions inside the ballast volume and not to the ambient environment.

Expression (1) can be written as;

$$L = K \frac{m(O_3)}{m(\text{air})} \frac{dm}{dt} = KQ \frac{dm}{dt}\quad (4)$$

where,

K = proportionality factor, including sensitivity of the detector.

$Q = m(O_3)/m(\text{air})$ = mass mixing ratio of ozone and air.

Using equation (3), equation (4) becomes

$$L = KQ \frac{MV_b}{RT_b} \left[\frac{dP_b}{dt} - P_b \frac{d(\ln T_b)}{dt} \right]. \quad (5)$$

Since T_b is very nearly constant, and is known by measurement, it is convenient to write equation (5) as:

$$L = K'Q \frac{dP}{dt} \quad (6)$$

where the subscript, b , is dropped and $K' = KMV_b/RT_b$ is a new constant. This equation simply states that the luminescence is proportional to the ozone mixing ratio times the rate of pressure change in the ballast volume.

DESCRIPTION OF OZONE SONDE

A picture of the ozone sensor is shown in figure 2 and a block diagram in figure 3. The ambient air is "drawn in" at the inlet port past the light baffle to exclude external light from the photometer. The inlet pipe is designed such that its conductance is high, the time constant being less than one second. The air is sampled by the chemiluminescent detector, which is made up of rhodamine-B dye absorbed on a porous Vycor substrate (NASA Tech Brief, 1965 and Parametrics Final Report, 1966). The luminescence is monitored by photometer consisting of a photomultiplier with an S-20 response, a light chopper, and A.C. amplifier. A small reference lamp is lighted near the photomultiplier every 40 seconds to give a calibration signal at the photometer output. The sampled air then empties into the ballast chamber. Attached to this chamber are two diaphragm-type pressure transducers whose ranges are 0-5 mm -Hg and 0-100 mm -Hg. A thermistor is also mounted on the chamber housing to indicate the temperature.

Each sensor output (0-5 volts) is fed to a quarter watt 234.0 Mc/s telemetry system using turnstile antennae. The telemeter includes 10 voltage controlled

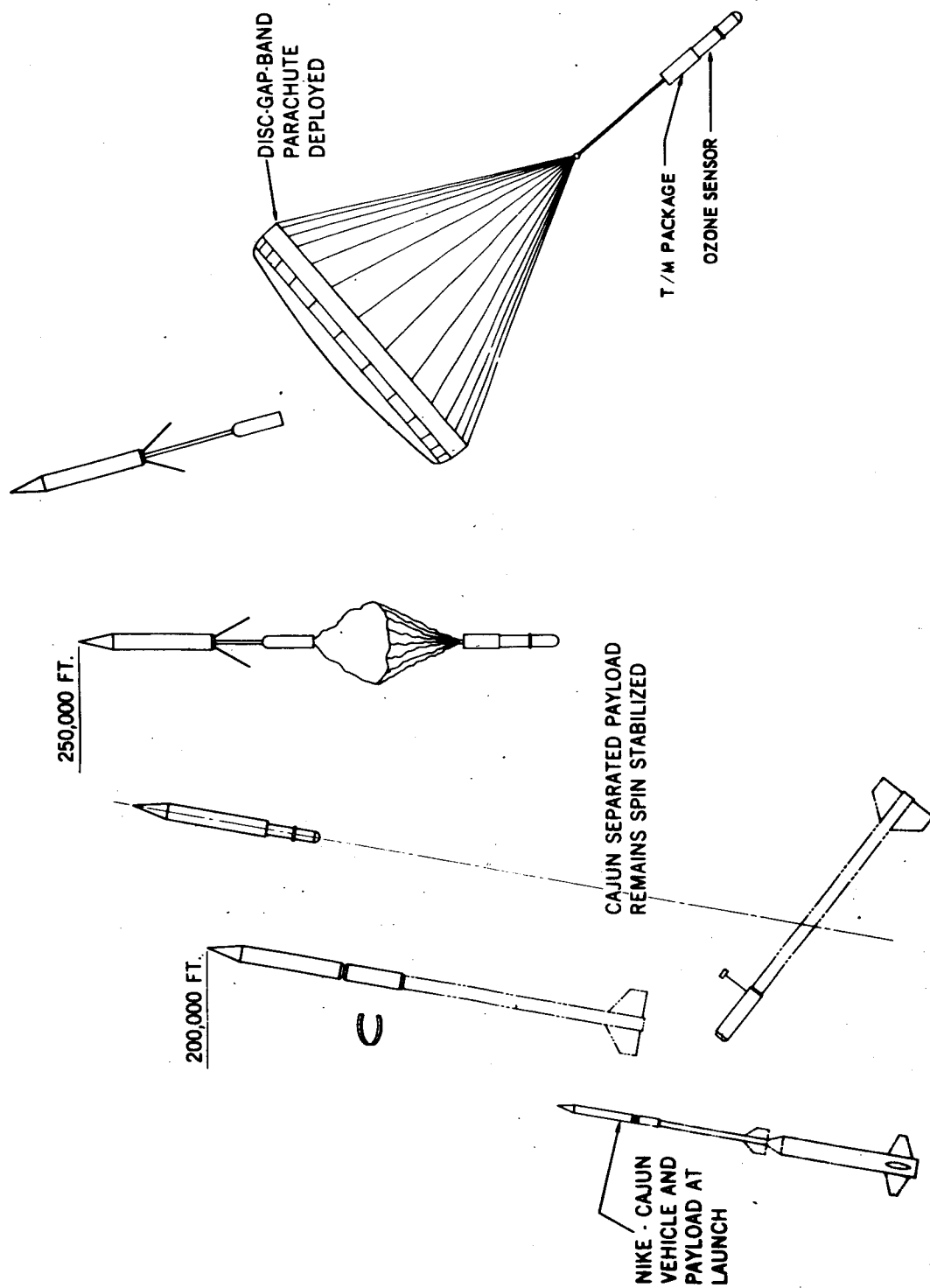


Figure 4-Flight Sequence of Events

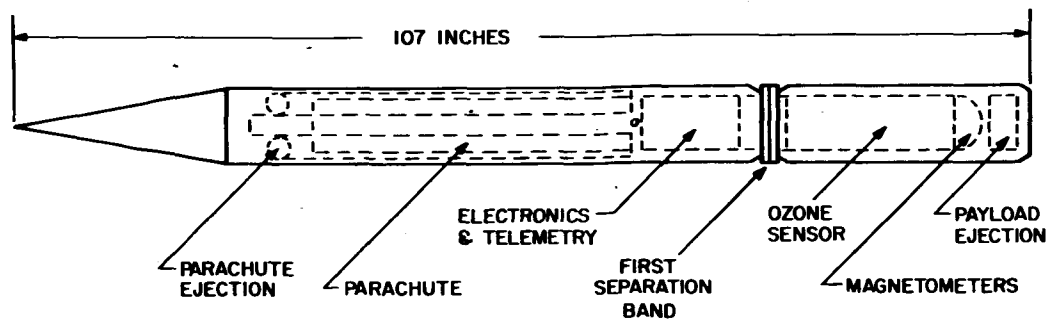


Figure 5-Payload Assembly

the linear dependence of ozone flux and luminescence, it is desirable to simulate flow rates, pressures, and ozone quantities expected during an actual flight. This simulation also provides for the preflight calibration.

From the expected descent rate of the parachute, dh/dt , and from the hydrostatic equation, $dp/dh = -\rho(h)g$, g one can write

$$\frac{dp_f}{dt} = -\rho(h) g \frac{dh}{dt} \quad (7)$$

the expected rate-of-change of the ambient pressure p_f encountered during descent. This profile is demonstrated by figures 6 and 7. A reproduction of $(dp/dt)_f$ in equation (7) by the ozone-simulator-calibrator is accomplished in the following manner (see figure 8). The calibrator is initially pumped down to less than 0.1 mm-Hg, while the ozone sensor inlet port is connected to the calibrator. Thus the ballast chamber is also pumped to the low pressure. When the low pressure is achieved the pump is blocked off from the system. Air is pumped past the ozone generator, a pen-ray mercury lamp, at atmospheric pressure to a point where the air plus ozone is allowed to enter the low pressure region of the calibrator through the needle valve, L_1 . At this point the air is sampled for ozone content by a Mast-Brewer electrochemical ozone meter (Brewer and Melford, 1960). The calibration begins when L_1 is opened and the volumes V_1 and V_2 fill with air plus ozone via a calibrated capillary leak, the ozone mixing ratio remaining constant throughout the calibration process. The volumes V_1 , V_2 , and leaks L_1 , and L_2 are chosen such that the pressure rise in V_2 matches dp_f/dt in equation (7) (Parametrics, 1966). The pressure rise in the ozone sensor ballast chamber and the photometer responses are monitored during the calibration which lasts approximately 10 minutes. This process corresponds

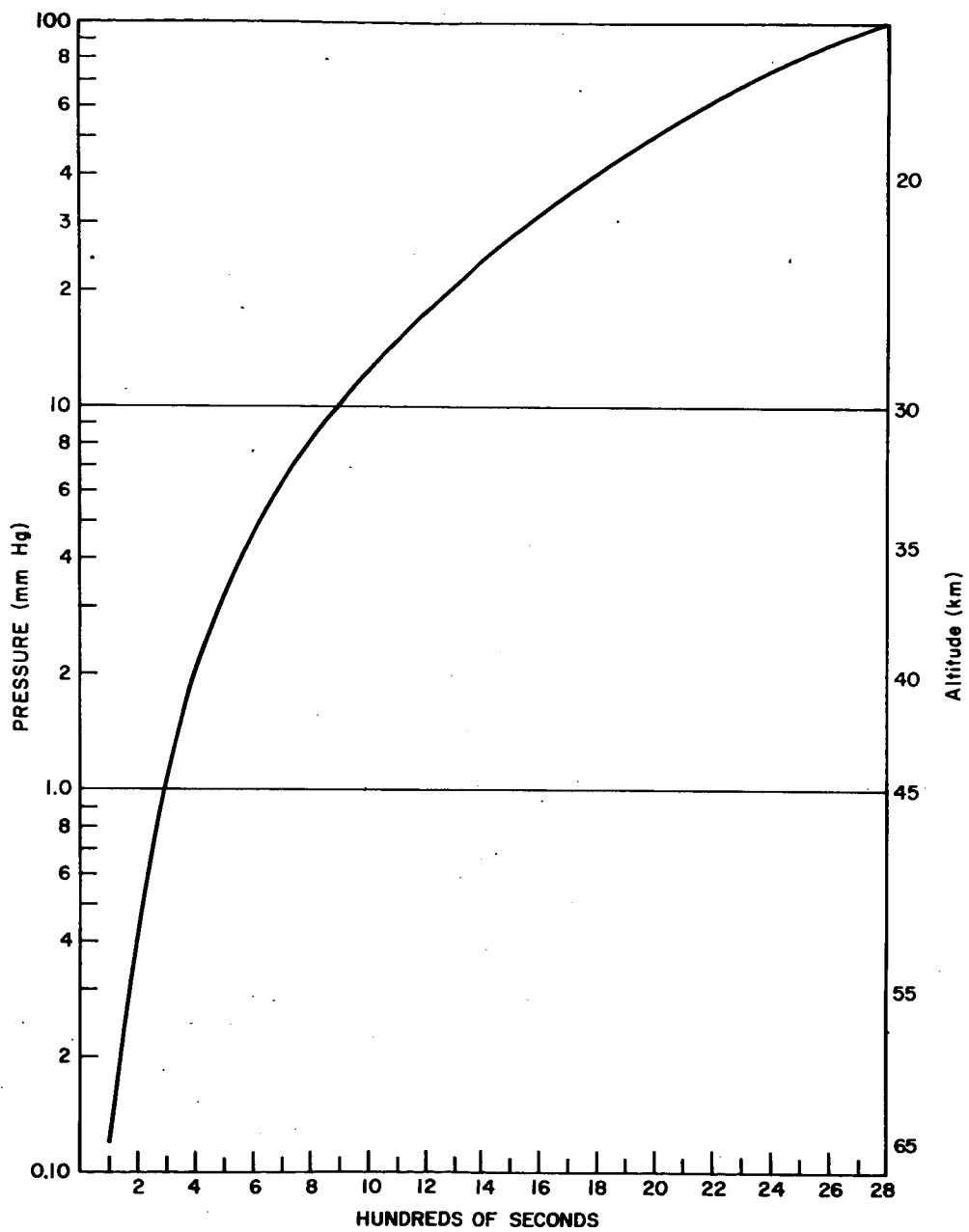


Figure 6—Ambient Pressure vs Descent Time

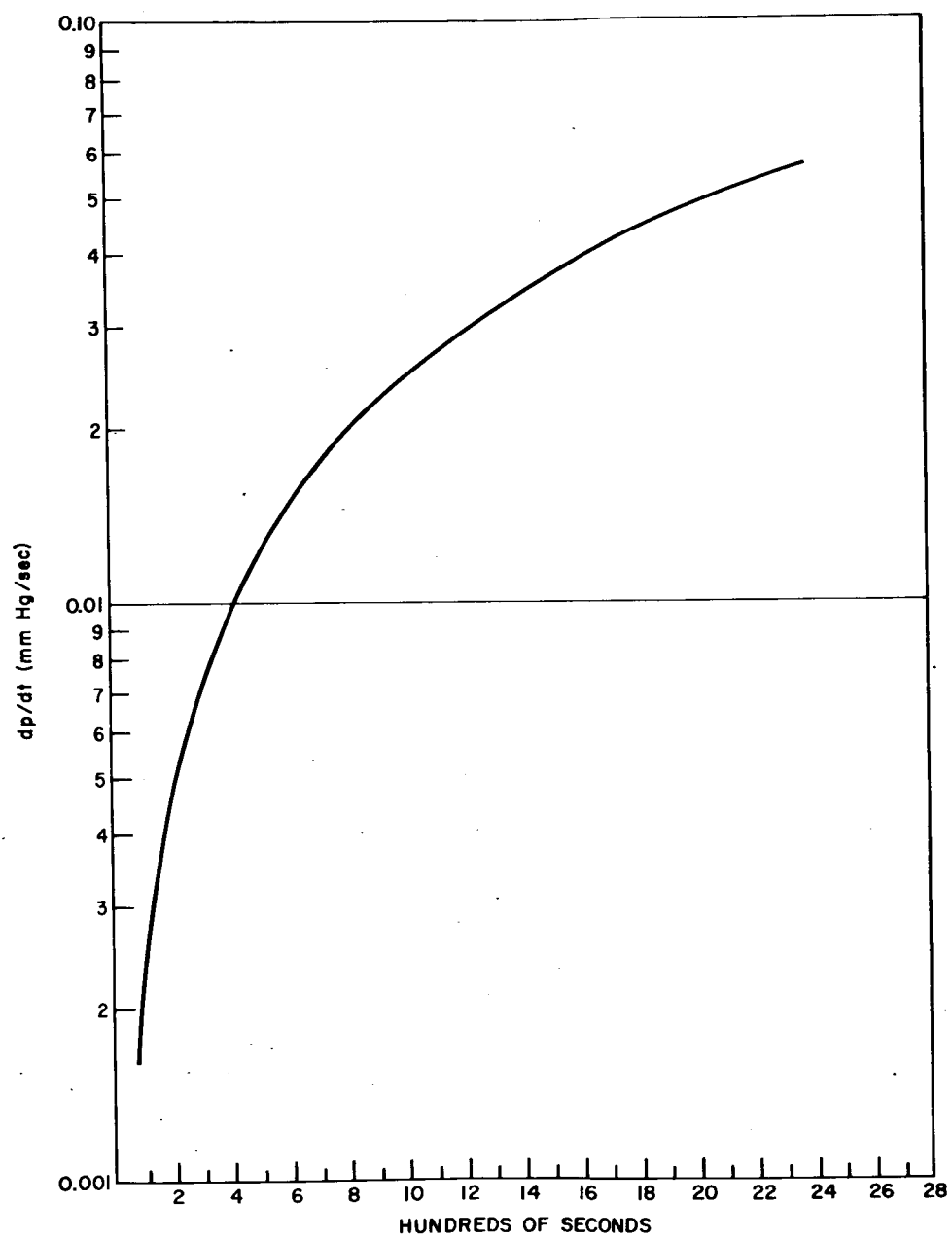


Figure 7—Rate of Change of Ambient Pressure vs Descent Time

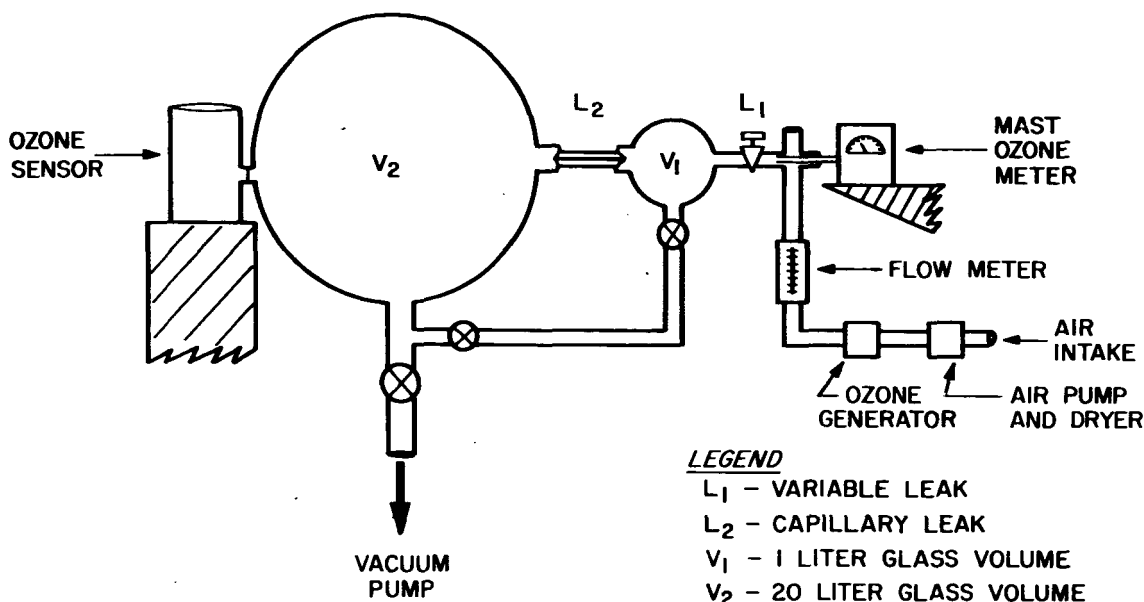


Figure 8—Ozone Sensor Simulator and Calibrator

to a parachute drop from approximately 70 km to approximately 30 km. The slope of plot of luminescence vs dp/dt at a fixed ozone mixing ratio yields the calibration constant of the ozone sensor, by equation (6).

THE INITIAL FLIGHT

The first ozone sonde was launched at White Sands Missile Range (WSMR) at 4:00 A.M. (MST) on December 9, 1966. Predicted apogee was 70 kilometers and the descent time approximately 120 minutes. Although the powered portion of the flight appeared to be normal, peak altitude was apparently lower than predicted. First separation and ejection of the payload from the second stage occurred on schedule, thus exposing the ozone sonde to the ambient atmosphere. The payload remained relatively stable, to apogee where second stage separation was to occur releasing the payload and parachute from the nosecone. However this did not happen until the payload had fallen to approximately 10 km. Telemetry data and examination of the recovered payload did indeed indicate parachute deployment. Since the falling payload reached terminal velocity, the parachute shredded upon deployment.

Throughout the flight the ozone sonde operated normally. However, an ozone profile was not measured since ozone fluxes into the sensor, due to the high descent rates, far exceeded those expected. A brief measurement of ozone mixing

ratio was accomplished just over apogee where descent rates were still not excessive. Unfortunately, ground radar lost the vehicle soon after launch, therefore, no apogee or descent data are available. Data from the pressure transducers indicated that apogee occurred at approximately the predicted time. However, peak altitude was about 20 km. lower than predicted. Magnetometer data indicated a change in orientation of the payload roll axis and some coning after first separation. This could have introduced additional drag thus lowering apogee. The magnetometer data also indicated that the initial induced roll was superimposed on the coning motion throughout the descent. This was of interest because pressure data qualitatively followed the payload motions. This may indicate that dynamic pressures may have a stronger effect on the flow rates than expected. However, pressure variations due to payload motions will not be as large if the parachute is properly deployed.

A probable cause of the failure of the parachute to be deployed has been determined from an examination of the backup payload. It is believed that a portion of a wire harness became bound on a row of screws holding the nosecone on the outer cylinder of the payload. It appears that deployment finally occurred due to the tumbling of the payload as it descended.

On December 4th and 5th, three ozone balloon measurements were successfully performed to approximately 30 kilometers at WSMR by Air Force Cambridge Laboratory personnel in support of this flight. Had the rocket flight been successful, an additional balloon ozone measurement and a Dobson total ozone measurement would have been performed at Albuquerque, New Mexico on December 9th. Arcsonde and radiosonde data for temperature, pressure, density, and winds at WSMR to 60 kilometers would also have been available on the launch date.

RESULTS

Since the payload fell freely from apogee, little useful data was taken. Maximum flow rates occurred about 25 seconds after apogee and the photometer channels saturated soon after that. Therefore, this analysis is directed toward the first 25 seconds after apogee.

It is of interest to compare a calculated flow rate to that measured by the sonde. The flow rate can be calculated from the equation of a freely falling body and the hydrostatic equation

$$\frac{dh}{dt} = -gt; \quad \frac{dp}{dh} = \frac{-P}{H}$$

therefore

$$\frac{dp}{dt} = \frac{dh}{dt} \frac{dp}{dh} = \frac{g p t}{H}$$

Where

h = height

t = time from apogee

g = acceleration due to gravity

p = pressure

H = scale height

The calculated values of dp/dt did not agree well with those measured by the sonde. This can not be explained by aerodynamic drag because calculated dp/dt values exceeded those measured. This discrepancy could be due to errors in the pressure measurement at these low pressures (near apogee), an aerodynamic affect since the sonde was rolling and coning, or the pressure in the ballast chamber did not reach equilibrium with the ambient pressure because of the lower than expected apogee.

Two determinations of ozone mixing ratio were made by averaging data between 0-15 seconds and 15-25 seconds after apogee, since definite trends of photometer signals and flow rates occurred over these intervals. Apogee was fixed at 60 kilometers from the pressure transducer data, therefore the above time intervals refer to altitudes of 59 and 57 kilometers respectively. It is reasonable to assume constant mixing ratio in these intervals. Therefore a curve of $L/(dp/dt)$ was constructed over these intervals and was compared to the preflight calibration. The curve of $L/(dp/dt)$ resulted in two straight lines of different slopes over each interval (which is reasonable) but still involved averaging over the few available data points. The error in dp/dt , or flow rate, is as high as 25%. The error in calibration is about 10%. The calculated ozone mixing ratio at 59 kilometers is .80 micrograms/gram and at 57 kilometers is 1.9 micrograms/gram. The altitude is not known to be better than ± 5 kilometers. Standard values of ozone at this altitude are given as 1.0-2.0 micrograms/gram and a few measurements give values as high as 10-20 micrograms/gram. A comparison of this ozone measurement with other data is given in figure 9.

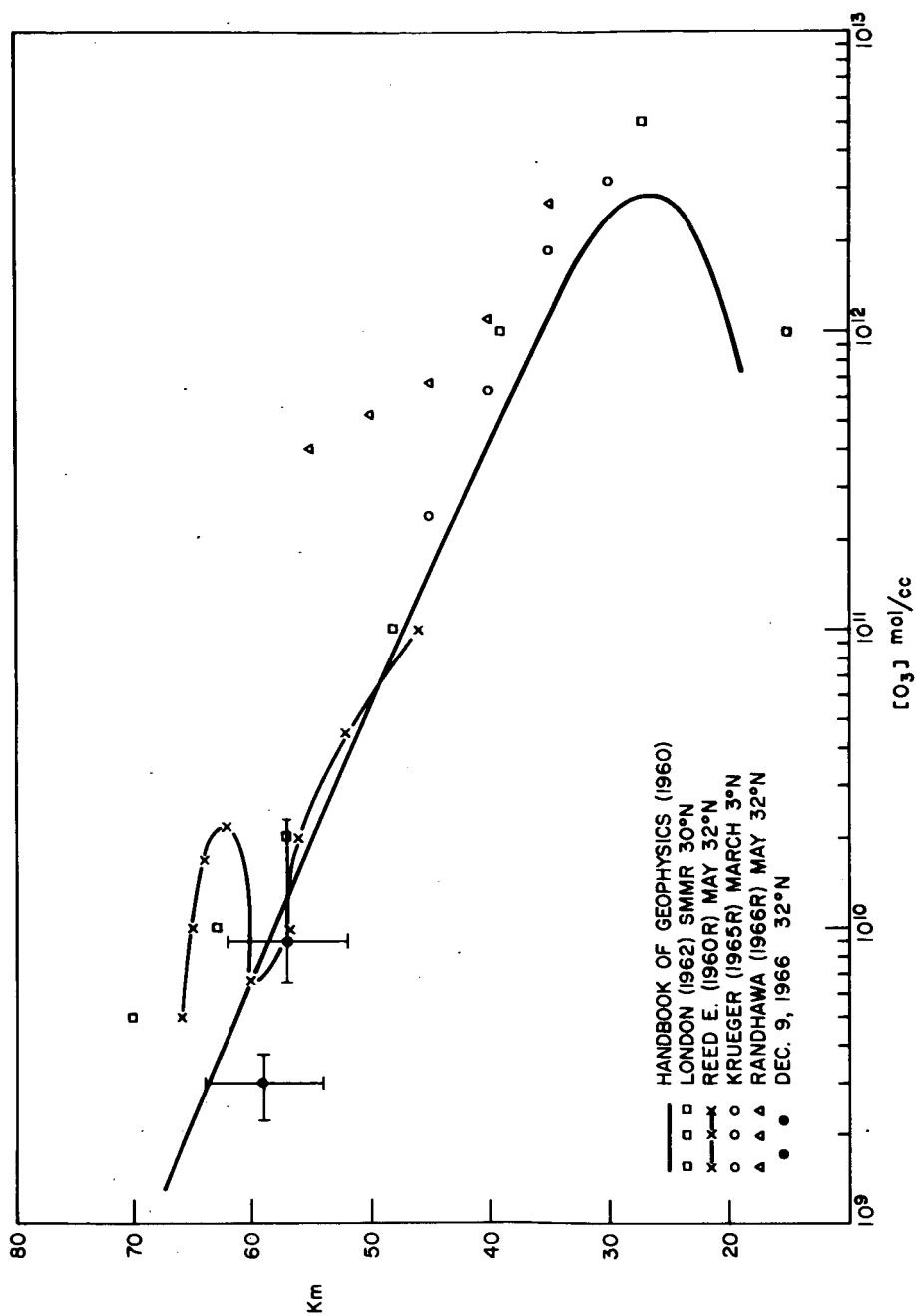


Figure 9—Comparisons of Ozone Concentrations vs Altitude

CONCLUSIONS

Though the flight of December 9 was not a success, the ozone sensor itself operated as intended and yielded measurements during the brief interval when the descent rates were within design limits. One of the primary objectives of the flight was not achieved, that is the determination of the stability of the descending parachute and what affect, if any, it would have on the self pumping mechanism. Magnetometer data gave some insight into this problem and will be of significance in future flights.

In order to determine the flow rate more easily, a suitable electronic differentiation of the pressure signal will be performed in future flights. This differentiated signal and the raw pressure data will both be telemetered during the descent.

A tone ranging system (a doppler technique) used in conjunction with the telemeter will be incorporated into future payloads for independent tracking of the payload. This system will not only provide a backup for the radar, but also allow for tracking at stations with no radar.

Throughout the calibrations, preflight checks, and final preflight calibration, the ozone sensor demonstrated excellent stability in regard to ozone sensitivity and showed that these sensitivities were high enough to measure the lowest concentrations. The confidence, thus gained, is important because problems of this type often seem to go hand in hand with measurements of "minor" constituents in the atmosphere.

REFERENCES

- Brewer, A.W. and J. R. Milford, Proceedings of the Royal Society, Vol. 256, 470-495, 1960.
- Hering, W.S. and T. Borden, "Mean Distribution of Ozone Density Over North America, 1963-1964," AFCRL 65-913, Environmental Research Paper No. 162, Dec. 1965.
- Murrow, H. W. and C. V. Eckstrom, "Description of a New Parachute Designed for Use with Meteorological Rockets," presented at the AIAA/AMS 6th National Conference on Applied Meteorology, Los Angeles, Calif., 1966.
- NASA Tech. Brief, Serial No. 65-10364, 1965.
- Parametrics, Inc., 1963, Final Report Contract NAS 5-2611, July 1963.
- Parametrics, Inc., 1966, Final Report Contract NAS 5-3638, July 1966.